

Role of Marine Biology in Glacial-Interglacial CO₂ Cycles

Karen E. Kohfeld,^{1*}† Corinne Le Quéré,^{1,‡} Sandy P. Harrison,^{1,§} Robert F. Anderson²

It has been hypothesized that changes in the marine biological pump caused a major portion of the glacial reduction of atmospheric carbon dioxide by 80 to 100 parts per million through increased iron fertilization of marine plankton, increased ocean nutrient content or utilization, or shifts in dominant plankton types. We analyze sedimentary records of marine productivity at the peak and the middle of the last glacial cycle and show that neither changes in nutrient utilization in the Southern Ocean nor shifts in plankton dominance explain the CO₂ drawdown. Iron fertilization and associated mechanisms can be responsible for no more than half the observed drawdown.

The causes of the 80- to 100-ppm atmospheric CO₂ fluctuations during glacial cycles remain elusive despite more than 20 years of research (1). Oceanic processes must account for the observed 80- to 100-ppm drawdown, as well as an additional 10 to 45 ppm resulting from decreased terrestrial carbon storage during glacial periods compared with interglacial periods (2). Current climate models are unable to reproduce the observed decrease in glacial atmospheric CO₂ using physical mechanisms alone (3), so changes in marine biology are often invoked as an additional mechanism to lower atmospheric CO₂. One family of explanations invokes changes in the sequestration of carbon in the deep ocean and ocean sediments resulting from the sinking of marine plankton and its detritus because of (i) iron fertilization of marine biota from increased atmospheric dust deposition to the ocean (4) and subsequent redistribution of limiting nutrients (5), (ii) increases in the oceanic nutrient content or the carbon/nitrogen/phosphorus (C/N/P) ratio (6), (iii) shifts in the dominant plankton types (7), and (iv) increased carbon and nutrient utilization in surface waters due to increased stratification (particularly in polar oceans) (8). Each of these processes is likely to affect specific oceanic regions and leave distinct imprints on the marine sediment record (Table 1). Here, we describe the various processes by

which the marine biological pump could have changed, identifying the oceanic regions they are likely to affect and the signature they would leave in marine sediments. We evaluate each process by examining the global reconstructions of marine activity archived in the paleoceanographic record.

Both the iron-fertilization and the increased-nutrient hypotheses require an increase in export production, or the amount of carbon exported to the seafloor. According to the iron-fertilization hypothesis (4), an increased supply of iron-rich dust to the oceans during glacial periods could have alleviated the iron limitation observed in high-nutrient, low-chlorophyll (HNLC) regions. The process of iron fertilization has been observed to increase carbon fixation in surface waters today (9–12). Although these

studies have not firmly established that iron fertilization increases export production, this process has been invoked as a means of increasing carbon flux to the deep ocean under conditions of high dust (4). This would have the strongest impact on the North Pacific, equatorial Pacific, and Southern Oceans (Fig. 1) and would be observed as higher dust-deposition rates and increased carbon and biogenic fluxes to marine sediments.

The increased-nutrient hypothesis suggests that carbon fixation and removal from surface waters could increase if the nutrient content of the whole ocean were increased or if the amount of carbon fixed per unit of nitrate and phosphate were greater (6, 13). This process was initially proposed to address nutrient limitation in warm low- to mid-latitude regions but would affect any oceanic region where nutrients are limiting (Fig. 1) and would be observed as increased carbon and biogenic fluxes to marine sediments.

Although dictated by slightly different processes, the first two hypotheses both predict increases in export production. What does the sediment record show? Changes in export production have been inferred from the fluxes of specific biogenic components (organic carbon, biogenic opal, and alkenone biomarkers), from naturally occurring radionuclides (²³¹Pa and ¹⁰Be), and from degradation products (barium, authigenic uranium, and/or cadmium) (14). None of these indicators provides an unequivocal signal, because the relationship between productivity and flux is influenced by multiple environmental factors. We have adopted an approach that assumes that changes in

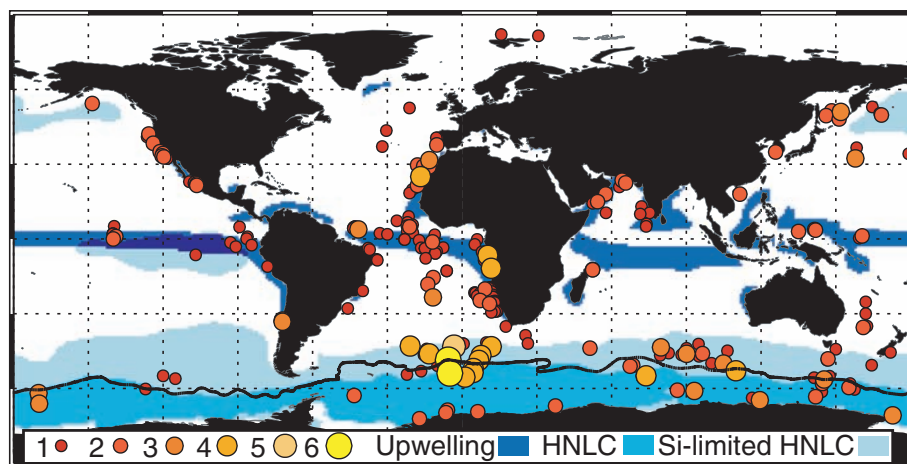


Fig. 1. Locations of ocean regions that are most critical for controlling uptake and sequestration of CO₂, including areas of wind-induced upwelling with annual values greater than 10 cm d⁻¹ (dark blue) (52); HNLC regions where either N/chl or P/chl is above 20 μmol/kg per mg Chl/m³, for an N/P ratio of 16 (intermediate blue); and HNLC regions with silica concentrations less than 20 μmol/kg per mg Chl/m³ (light blue). Nutrient data are from (53). Solid line shows approximate location of the APF (54). Overlaid dots show locations of cores that provide estimates of changes in export production used in this study. The size of the overlaid dots indicates the number of export-production indicators available per core.

¹Max Planck Institute for Biogeochemistry, Jena, Germany. ²Lamont-Doherty Earth Observatory and Department of Earth and Environmental Sciences, Columbia University, Palisades, NY 10964, USA.

*To whom correspondence should be addressed. E-mail: office@kohfeld.com

†Present address: School of Earth and Environmental Sciences, Queens College of City University of New York, Flushing, NY 11367, USA.

‡Present address: University of East Anglia and the British Antarctic Survey, UK.

§Present address: School of Geographical Sciences, University of Bristol, Bristol, UK.

any specific indicator reflect changes in export production if several other indicators imply the same change. Carbonate accumulation responds more strongly than other indicators to chemical feedbacks associated with changes in ocean carbonate chemistry, as well as being affected by preservation overprints associated with deepwater circulation (3). It is therefore excluded from our overall assessment of changes in export production. We assess the relative change in export production between different time intervals using a five-point scale (lower, slightly lower, no change, slightly higher, and higher) (15). We evaluate the reliability of these qualitative assessments at each site on the basis of the quality of the age model and measurement methods, the number of sedimentary indicators, and the degree of consensus between them (15).

We obtained estimates of the change in export production (i) between the last glacial maximum (LGM) (~18,000 to 22,000 years ago) and the late Holocene (about the last 5000 years, which we use to define the modern state) from 258 cores; (ii) between marine isotope stages 5a to 5d (stage 5a-d) (80,000 to 110,000 years ago) and the LGM from 83 cores; and (iii) between stage 5a-d and the late Holocene from 80 cores. Stage 5a-d is a period when atmospheric CO₂ levels were ~50 ppm lower

than late Holocene levels, but atmospheric dust deposition to the ocean was close to present-day levels (16–21) compared with the deposition rates observed during the LGM (22), which were two to three times as high. Long time-series records of dust deposition to the ocean demonstrate that the relatively low dust influx was not only observed in the Vostok ice core (23) but also represented a global phenomenon (fig. S1). Stage 5a-d therefore allows us to determine the impact of export production on atmospheric CO₂ in the absence of enhanced iron fertilization due to dust. We use the Holocene as an analog for the last interglacial period, stage 5e (130,000 to 115,000 years ago), assuming that Holocene conditions are representative of those that existed during stage 5e. We base this assumption on the fact that the change in external forcing (i.e., solar insolation) compared with the present was in the same direction during both periods (24). As a result, many regional climate changes affected by seasonal and latitudinal insolation patterns are likely to have occurred during both periods. Furthermore, the Vostok ice-core record reveals that the past four interglacial periods experienced very similar atmospheric CO₂ levels (23). Thus, we assume that conditions of the global carbon cycle must have been similar from one interglacial period

to the next to have produced such consistency among peak interglacial CO₂ levels.

Export production during stage 5a-d is lower than during the late Holocene in the western Pacific, the South Atlantic gyre, the eastern Atlantic, and the Southern (south of 50°S) Oceans (Fig. 2A). The upwelling region in the eastern equatorial Atlantic and the present-day Antarctic Polar Front (APF) show slightly higher export production at stage 5a-d compared with the Late Holocene. These areas are relatively small and do not affect the overall picture that global export production was lower during stage 5a-d than during the late Holocene. Export production was globally higher during the LGM than during either stage 5a-d or the Late Holocene (Fig. 2, B and C). Only the Southern Ocean, south of the modern-day APF, had lower export production at the LGM than in the late Holocene or stage 5a-d. The northwest Pacific, the subantarctic, and equatorial regions of the Atlantic and Indian Oceans were all characterized by increased export production at the LGM. Export production to the north of the modern-day APF was higher during stage 5a-d than during the late Holocene, and this increase was further enhanced during the LGM. This suggests that changes in export production had already begun during stage 5a-d in the

Table 1. Mechanisms by which marine biota can reduce atmospheric CO₂ concentrations.

Hypothesis	Description	Oceanic regions influenced	Sediment impact (LGM compared to modern)	Ref.
Iron fertilization	Increased inputs of iron-rich dust increase marine productivity, carbon uptake in surface waters, and subsequent carbon flux to the deep ocean, which lowers atmospheric CO ₂ .	Regions influenced by eolian dust input and with underutilized nutrient (P, N, Si) inventories (Southern Ocean, North Pacific, equatorial Pacific).	Increased dust accumulation rates, increased accumulation of exported carbon.	(4)
Whole-ocean nutrient increase	Increased ocean nutrient reservoir alleviates nutrient limitation and allows global increase in marine biomass and carbon export to deep ocean.	Nutrient-limited regions (e.g., low-latitude gyres).	Increased export carbon flux globally.	(6, 13)
Nutrient utilization	Increased utilization of carbon and nutrients in surface waters removes CO ₂ from contact with the atmosphere and results in lower atmospheric CO ₂ . Increased nutrient utilization could occur either by increasing surface production or by decreasing vertical mixing and, therefore, the supply of nutrients and CO ₂ to surface waters.	Regions with underutilized nutrient inventories (primarily the Southern Ocean, equatorial Pacific, and North Pacific, with the Southern Ocean containing a majority of unused nutrients and having a strong connection with CO ₂ -rich deep waters).	Higher nitrate uptake (increased ¹⁵ N of organic material in surface waters); lower surface-water phosphate concentrations (lower Cd/Ca ratios in planktonic foraminifera); higher surface-water silica uptake (increased δ ³⁰ Si in diatoms); lower surface-water CO ₂ concentrations (relative increase in δ ¹³ C of organic material).	(8)
CaCO ₃ /Corg rain ratio	Decreased export of CaCO ₃ relative to organic carbon from surface to deep ocean maintains high surface-water alkalinity (CO ₂ more soluble) and reduces deep-ocean carbonate burial. Associated whole-ocean alkalinity increase reduces atmospheric CO ₂ .	Mainly in regions dominated by coccolithophorid production today but a global shift expected.	Relative decrease in calcite-producing plankton; whole-ocean increase in carbonate preservation.	(7)
Silica leakage	Mechanism by which the rain ratio could change. Iron-fertilized diatoms in the Southern Ocean take up less silicic acid relative to nitrate. The unused silicic acid is exported to silicon-limited regions, increases diatom production at the expense of coccolithophorids, and decreases the CaCO ₃ to organic carbon rain ratio.	Regions north of the APF that are silicon limited. Low latitudes influenced by mixing of subantarctic mode water into the thermocline.	Shift from calcite- to silicate-producing plankton; increased export production; increased deep-ocean alkalinity (whole-ocean increase in carbonate preservation; increased carbonate-ion content).	(5, 32)

region of the modern-day APF, although the full increase was not realized until the LGM.

Figure 2 shows that export production decreased at the beginning of the glaciation (Fig. 2A, stage 5a-d minus late Holocene) and increased subsequently (Fig. 2B, LGM minus stage 5a-d) and increased subsequently (Fig. 2C, LGM minus stage 5a-d). Thus, the 50-ppm drawdown that

had occurred by stage 5a-d cannot be explained by increased export production resulting from increased nutrient content or changes in the C/N/P ratio. Increased export production during the LGM is synchronous with the observed maximum in dust concentration, thus lending support to the hypothesis of iron fer-

tilization during glaciations. It is possible that iron fertilization could explain the last 30 to 50 ppm of atmospheric CO_2 drawdown during the glacial period. This is consistent with the observation that when an ocean-biogeochemistry model is forced to reproduce the observed LGM export-production patterns, there is only a slight increase in global export production (+6% or +0.7 PgC/year) (14). In this experiment and in other simulations, iron fertilization accounts for <40-ppm decrease in atmospheric CO_2 (3, 14, 25).

Increased surface-water nutrient and carbon utilization through the biological pump could also explain atmospheric CO_2 drawdown. This process could be particularly important in the Southern Ocean because of the large inventory of unused surface nutrients and the strong connection between surface waters and CO_2 -rich deep waters. Increased nutrient utilization would occur if decreased vertical mixing south of the APF reduced the supply of nutrients and CO_2 to surface waters (1, 8, 26). Increased nutrient utilization south of the modern-day APF at the LGM compared with the late Holocene would bring about higher nitrate uptake, resulting in increased ^{15}N of organic material in surface waters (8); lower surface-water phosphate concentrations, causing lower Cd/Ca ratios in planktonic foraminifera (27); higher surface-water silica uptake, resulting in increased $\delta^{30}\text{Si}$ (28); and lower surface-water CO_2 concentrations, resulting in a relative increase in $\delta^{13}\text{C}$ of organic material (29). LGM records from south of the modern-day APF (fig. S2) do show higher $\delta^{15}\text{N}$ values, but proxy records indicate that phosphate concentrations (foraminifera Cd/Ca ratios) are higher, silica utilization ($\delta^{30}\text{Si}$) is lower, and surface-water CO_2 concentrations (organic $\delta^{13}\text{C}$) are higher than late Holocene values. Three of the four surface ocean indicators ($\delta^{13}\text{C}$, Cd/Ca, and $\delta^{30}\text{Si}$) are consistent with both a decrease in nutrient utilization and the observed decrease in export production. Recent improvements in measurement techniques have called the reliability of existing $\delta^{15}\text{N}$ data into question (30), so it is possible that future $\delta^{15}\text{N}$ data will prove more consistent with other nutrient indicators. Although we recognize that all of these paleonutrient indicators are affected by environmental factors that complicate their interpretation (31), the balance of evidence does not support the view that nutrient utilization accounted for a substantial part of the atmospheric CO_2 drawdown south of the modern-day APF.

The final explanation for changes in the marine biological pump invokes a shift in the dominant plankton types that would have decreased the export of carbonate relative to organic carbon (the rain ratio), resulting in an increase in the carbonate-ion content of seawater and thereby drawing down atmospheric CO_2 (7). Decreasing the relative export

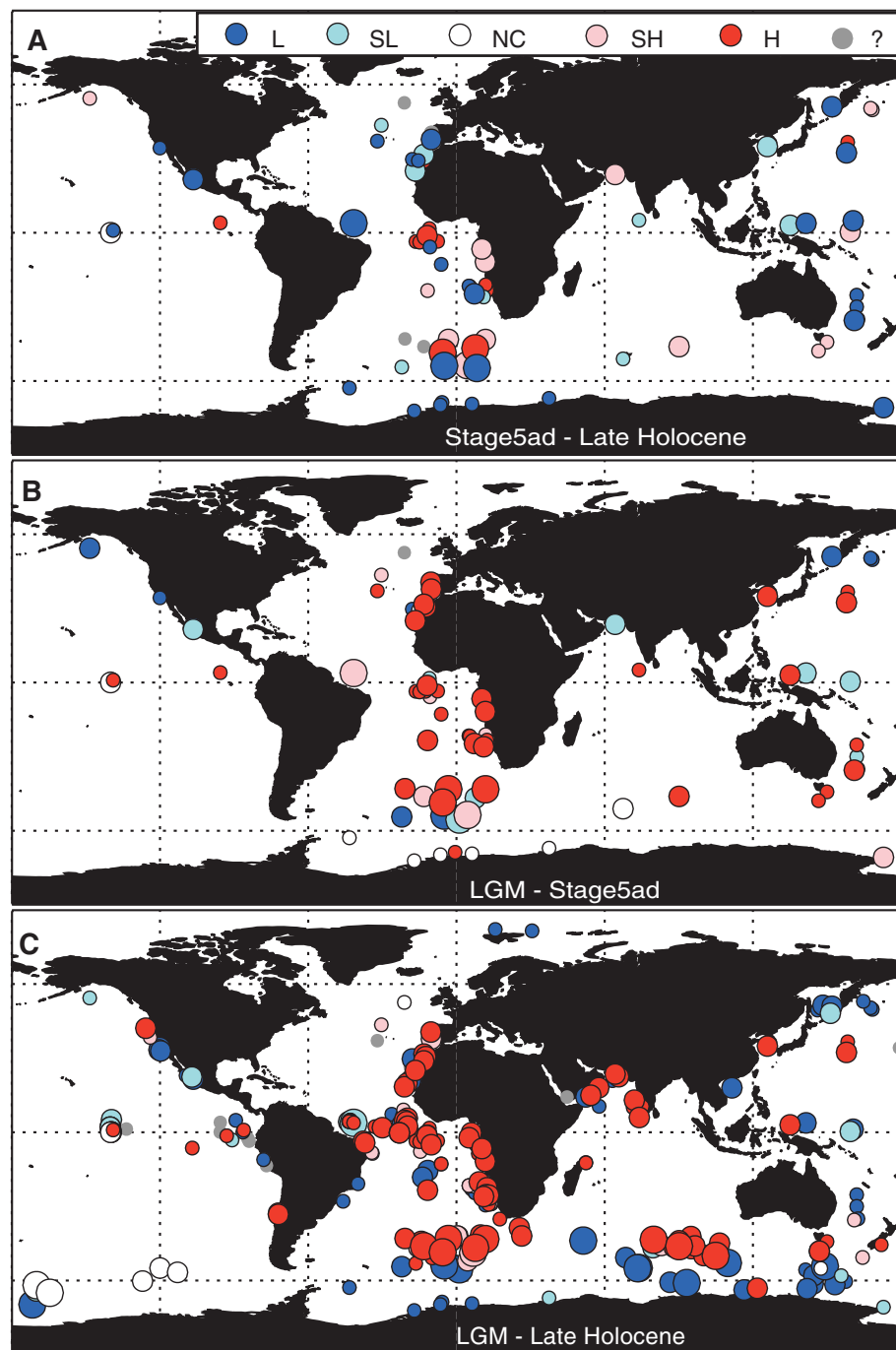


Fig. 2. Relative changes in export production for (A) stage 5a-d (80,000 to 110,000 years ago) minus Late Holocene (0 to 5000 years ago), (B) LGM (18,000 to 22,000 years ago) minus stage 5a-d, and (C) LGM minus Late Holocene. Dark and pale blue circles indicate lower (L) and slightly lower (SL) export production, respectively; dark and pale red circles indicate higher (H) and slightly higher (SH) export, respectively. White circles indicate no change (NC) between the two time periods. Gray circles represent sites where there is no unambiguous consensus between the different types of data. The size of the circle indicates the level of confidence (with small circles indicating low and large circles high confidence) in the assessment of the change in export production (15).

of calcium carbonate to the seafloor could occur as a result of a global shift from primarily carbonate-producing plankton to siliceous (or other noncarbonate-producing) plankton. A mechanism that both decreases the rain ratio and reconciles the $\delta^{15}\text{N}$ and $\delta^{30}\text{Si}$ records in the Southern Ocean has recently been proposed (5, 32), based on observations that diatoms take up substantially less silicic acid relative to nitrate under high-iron conditions (32, 33). The “silica-leakage” hypothesis suggests that increased deposition of iron-rich dust during the last glacial period could account for high nitrate utilization while still leaving a pool of unused silicic acid in the Southern Ocean. This excess silicic acid could have been transported to the subantarctic and then to low-latitude thermocline waters by subantarctic mode waters. This would alleviate silicon limitation in both the subantarctic and the low-latitude HNLC regions (Fig. 1), thereby increasing diatom production at the expense of coccolithophorids.

The silica-leakage hypothesis would be registered as a shift from carbonate-producing to silicon-bearing plankton in marine sediments. Furthermore, the silica-leakage hypothesis constrains the timing and impact of this plankton shift to be coincident with increases in dust supply, and it would manifest itself as higher export production south of the APF. However, we have demonstrated that dust supply as well as export production in the Southern Ocean south of the APF were low during stage 5a-d compared with both the LGM and the late Holocene. Thus, the silica-leakage hypothesis as described above cannot be invoked to explain the initial 50-ppm decrease in atmospheric CO_2 .

Records measuring specific molecular biomarkers demonstrate a shift from coccolithophorid to diatom assemblages in the Tasman Sea (34, 35) and demonstrate that the contribution of coccolithophorids to the total flux of organic carbon in the South Atlantic (36), off northwest Africa (37, 38), and in the Arabian Sea (39) was less important at the LGM than it is today. However, the decrease in the contribution of coccolithophorids occurs at the peak glacial period, well after stage 5a-d. Therefore, although the number of records is limited and more data are needed, especially from HNLC regions where silicon is limiting (in the Pacific Basin, Fig. 1), existing results are consistent with the hypothesis that a shift in phytoplankton taxa may have contributed to the lowering of atmospheric CO_2 from stage 5a-d to the LGM but not to the initial lowering of atmospheric CO_2 from stage 5e to stage 5d.

Both the rain-ratio hypothesis and the silica-leakage hypothesis also predict increases in the overall carbonate-ion content of deepwater, as well as a global increase in carbonate preservation in marine sediments [see (1) for review]. Although benthic foraminiferal boron

isotope measurements of deepwater pH imply that carbonate-ion concentrations were 100 $\mu\text{mol/kg}$ higher at the LGM compared with today (40), several other measures suggest very different conditions: (i) reconstructions of carbonate burial rates suggest little or no deepening of the lysocline required by an increase in carbonate-ion concentration (41), (ii) increases in foraminiferal size imply that carbonate-ion concentrations were only 4 to 8 $\mu\text{mol/kg}$ higher (42), and (iii) foraminiferal assemblage dissolution indices estimate that carbonate-ion concentrations were a maximum of 5 $\mu\text{mol/kg}$ higher in the Pacific and 20 $\mu\text{mol/kg}$ lower in the Atlantic (43). Three of these four indicators suggest only a small change in deepwater carbonate-ion concentration. Thus, the evidence suggests that the expected change in deep-sea carbonate-ion concentration predicted by any form of the rain-ratio hypothesis is not observed.

We recognize limitations that could affect our conclusions. First, data coverage is poor in some regions, and nutrient utilization may occur in places other than the Southern Ocean. Figure 1 highlights key oceanic regions that remain relatively understudied with respect to the glacial-interglacial carbon cycle, and Fig. 2 demonstrates key regions where data do not agree. Second, vertical fluxes of biogenic components to the deep sea can be affected by other factors, such as sediment redistribution. Although we have corrected for these factors wherever possible (^{230}Th normalization was used in 77 out of 258 cores), further analyses may be needed to confirm our conclusions. Third, further research is required to improve our quantification of glacial-interglacial changes in deepwater carbonate-ion concentrations and carbonate burial. Finally, there may be interactions between physical and biological processes (such as the extent of vertical mixing and the impacts of interactive sea ice on polar biology) that might lead to a synergistic enhancement of the impact of ocean physics and biology on atmospheric CO_2 drawdown. Despite these potential limitations, our analysis shows that export production was low during stage 5a-d and increased afterward to reach its maximum at the LGM. Thus, we conclude that observational evidence does not support the idea that large-scale changes in the marine biological pump was the dominant influence on atmospheric CO_2 changes during glaciations.

Alternative hypotheses that can explain the initial 50-ppm decrease in atmospheric CO_2 without conflicting with biological data reconstructions include increased stratification of the glacial ocean (1, 44), reduced ventilation of CO_2 -rich deepwater resulting from increased sea-ice cover (45), and changes in the location and mechanisms of deepwater formation that alter deepwater composition (46). The first two mechanisms require that

actual vertical mixing in the ocean be much smaller than the effective vertical mixing currently observed in global ocean circulation models (47, 48); the third mechanism requires that ocean circulation models have stronger air-sea CO_2 equilibration in deepwater formation regions of the Southern Ocean than they do currently (49).

Current ocean general circulation models are unable to reproduce the observed variations in atmospheric CO_2 with the use of physical mechanisms alone; this is why the marine biological pump is often invoked as a probable mechanism to lower atmospheric CO_2 . Our data analysis suggests that ocean biology contributed less than half of the observed glacial-interglacial variations in atmospheric CO_2 and therefore that physical processes must be responsible for most of the oceanic uptake of atmospheric CO_2 during glaciations. Our analysis thus suggests that ocean models should be more sensitive to changes in climate than they are currently, a conclusion supported by their inability to reproduce observed decadal variations in oceanic heat (50) and oxygen content (50, 51).

References and Notes

1. D. M. Sigman, E. A. Boyle, *Nature* **407**, 859 (2000).
2. J. Kaplan, I. C. Prentice, W. Knorr, P. Valdes, *Geophys. Res. Lett.* **29**, 1079 (2002).
3. D. Archer, A. Winguth, D. Lea, N. Mahowald, *Rev. Geophys.* **38**, 159 (2000).
4. J. Martin, *Paleoceanography* **5**, 1 (1990).
5. K. Matsumoto, J. L. Sarmiento, M. A. Brzezinski, *Global Biogeochem. Cycles* **16**, 10.1029/2001GB001442 (2002).
6. W. S. Broecker, *Geochim. Cosmochim. Acta* **46**, 1689 (1982).
7. D. Archer, E. Maier-Reimer, *Nature* **367**, 260 (1994).
8. R. François et al., *Nature* **389**, 929 (1997).
9. A. Tsuda et al., *Science* **300**, 958 (2003).
10. P. W. Boyd et al., *Nature* **407**, 695 (2000).
11. K. H. Coale et al., *Science* **304**, 408 (2004).
12. K. H. Coale et al., *Nature* **383**, 495 (1996).
13. M. B. McElroy, *Nature* **302**, 328 (1983).
14. L. Bopp, K. E. Kohfeld, C. Le Quéré, O. Aumont, *Paleoceanography* **18**, 10.1029/2002PA000810 (2003).
15. Materials and methods are available as supporting material on Science Online.
16. H. Kawahata, K. I. Ohkushi, Y. Hatakeyama, *J. Oceanogr.* **55**, 747 (1999).
17. H. Kawahata, T. Okamoto, E. Matsumoto, H. Ujiie, *Quat. Sci. Rev.* **19**, 1279 (2000).
18. R. Tiedemann, M. Sarnthein, N. J. Shackleton, *Paleoceanography* **9**, 619 (1994).
19. S. C. Clemens, W. L. Prell, *Paleoceanography* **5**, 109 (1990).
20. S. Schneider, *Ber. Fachber. Geowiss. Universit. Bremen* **187**, 134 (2002).
21. P. P. Hesse, *Quat. Sci. Rev.* **13**, 257 (1994).
22. K. E. Kohfeld, S. P. Harrison, *Earth Sci. Rev.* **54**, 81 (2001).
23. J. R. Petit et al., *Nature* **399**, 439 (1999).
24. A. L. Berger, *Quat. Res.* **9**, 139 (1978).
25. A. J. Watson, D. C. E. Bakker, A. J. Ridgwell, P. W. Boyd, C. S. Law, *Nature* **407**, 730 (2000).
26. D. M. Sigman, M. A. Altabet, R. François, D. C. McCorckle, J.-F. Gaillard, *Paleoceanography* **14**, 118 (1999).
27. H. Elderfield, R. E. M. Rickaby, *Nature* **405**, 305 (2000).
28. C. L. De La Rocha, M. A. Brzezinski, M. J. DeNiro, A. Shemesh, *Nature* **395**, 680 (1998).
29. Y. Rosenthal, M. Dahan, A. Shemesh, *Paleoceanography* **15**, 65 (2000).
30. R. S. Robinson, B. G. Brunelle, D. M. Sigman, *Paleoceanography* **19**, PA3001 (2004); 10.1029/2003PA000996.

31. R. F. Anderson, Z. Chase, M. Q. Fleisher, J. P. Sachs, *Deep-Sea Res. II* **49**, 1909 (2002).
32. M. A. Brzezinski et al., *Geophys. Res. Lett.* **29**, 1564 (2002).
33. D. A. Hutchins, K. W. Bruland, *Nature* **393**, 561 (1998).
34. M. Ikehara et al., *Paleoceanography* **15**, 170 (2000).
35. E. Calvo, C. Pelejero, G. A. Logan, P. De Deckker, *Paleoceanography* **19**, 10.1029/2003PA000992 (2004).
36. P. J. Mueller, M. Cepek, G. Ruhland, R. R. Schneider, *Paleogeogr. Paleoclimatol. Paleocol.* **135**, 71 (1997).
37. M.-A. Sicre et al., *Org. Geochem.* **31**, 577 (2000).
38. P. Martinez et al., *Org. Geochem.* **24**, 411 (1996).
39. D. Budzjak et al., *Paleoceanography* **15**, 307 (2000).
40. A. Sanyal, N. G. Hemming, G. N. Hanson, W. S. Broecker, *Nature* **373**, 234 (1995).
41. N. R. Catubig et al., *Paleoceanography* **13**, 298 (1998).
42. J. Bijma, B. Hoenisch, R. E. Zeebe, *Geochem. Geophys. Geosys.* **3**, 10.1029/2002GC00038 (2002).
43. D. M. Anderson, D. Archer, *Nature* **416**, 70 (2002).
44. J. R. Toggweiler, *Paleoceanography* **14**, 571 (1999).
45. B. B. Stephens, R. F. Keeling, *Nature* **404**, 171 (2000).
46. J. R. Toggweiler, R. Murnane, S. Carson, A. Gnanadesikan, J. L. Sarmiento, *Global Biogeochem. Cycles* **17**, 1027 (2003).
47. D. E. Archer et al., *Paleoceanography* **18**, 10.1029/2002PA000760 (2003).
48. W. Broecker et al., *Global Biogeochem. Cycles* **13**, 817 (1999).
49. J. R. Toggweiler, A. Gnanadesikan, S. Carson, R. Murnane, J. L. Sarmiento, *Global Biogeochem. Cycles* **17**, 1026 (2003).
50. S. Levitus et al., *Science* **292**, 267 (2001).
51. L. Bopp, C. Le Quéré, M. Heimann, A. C. Manning, P. Monfray, *Global Biogeochem. Cycles* **16**, 1022 (2002).
52. L. Xie, W. W. Hsieh, *Fish. Oceanogr.* **4**, 52 (1995).
53. M. E. Conkright et al., *NOAA Atlas NESDIS 46 World Ocean Database 2001*, vol. 5, *Temporal Distribution of Nutrient Profiles* (U.S. Government Printing Office, Washington, DC, 2002).
54. A. H. Orsi, T. Whitworth, W. D. Nowlin, *Deep-Sea Res.* **42**, 641 (1995).
55. We thank A. Ridgwell, S. Kienast, I. Tegen, and two anonymous reviewers for helpful comments. We gratefully acknowledge the work of all authors cited in the Supporting Online Material for their invaluable data contributions. The ideas presented here emerged from stimulating discussions with I. C. Prentice and the participants of the Green Ocean Project: www.bgc-jena.mpg.de/bgc-synthesis/projects/green_ocean.

Supporting Online Material

www.sciencemag.org/cgi/content/full/308/5718/74/DC1
Materials and Methods
Figs. S1 to S5
Tables S1 to S3

17 September 2004; accepted 31 January 2005
10.1126/science.1105375

Getting to Know You: Reputation and Trust in a Two-Person Economic Exchange

Brooks King-Casas,¹ Damon Tomlin,¹ Cedric Anen,³
Colin F. Camerer,³ Steven R. Quartz,³ P. Read Montague^{1,2*}

Using a multi-round version of an economic exchange (trust game), we report that reciprocity expressed by one player strongly predicts future trust expressed by their partner—a behavioral finding mirrored by neural responses in the dorsal striatum. Here, analyses within and between brains revealed two signals—one encoded by response magnitude, and the other by response timing. Response magnitude correlated with the “intention to trust” on the next play of the game, and the peak of these “intention to trust” responses shifted its time of occurrence by 14 seconds as player reputations developed. This temporal transfer resembles a similar shift of reward prediction errors common to reinforcement learning models, but in the context of a social exchange. These data extend previous model-based functional magnetic resonance imaging studies into the social domain and broaden our view of the spectrum of functions implemented by the dorsal striatum.

The expression and repayment of trust is an important social signaling mechanism that influences competitive and cooperative behavior (1–6). The idea of trust typically conjures images of complex human relationships, so it would seem to be a difficult part of social cognition to probe rigorously in a scientific experiment. Nevertheless, instances of trust can be stripped of complicating contextual features and encoded into economic exchange games that preserve its essential features (7–9). For example, in a game in which two players send money back and forth with risk, trust is operationalized as the amount of money a sender gives to a receiver without external enforcement

(9). Such trust games now enjoy widespread use both in experimental economics (10) and neuroscience experiments (11–17).

To measure neural correlates of trust using functional magnetic resonance imaging (fMRI), we first made a simple modification to a single-exchange trust game in order to improve the ecological validity of the task (10). Specifically, we changed the single-round format to a multi-round format in which the same two individuals (one designated the “investor,” and the other the “trustee”) played 10 consecutive rounds. This modification reflects the fact that significant social exchanges are rarely single-shot, and the assumption that algorithms in our brains are tuned to this fact (1–6). Thus, by adapting the multi-round format, (i) trust becomes bidirectional, in that both the investor and trustee assume the risk that money sent might not be reciprocated by their partner; and (ii) reputation building can be probed, as players develop models of one another through iterated exchange (10, 11). Participants were informed that individual rounds of

the trust game would be implemented as follows: One player (investor) could invest any portion of \$20 with the other player (trustee), the money appreciated (three times the investment), and the trustee then decided how much of the tripled amount to repay (Fig. 1) (18). Players maintained their roles throughout the entire 10-round game. Responses were encoded only in monetary units and player identities were never revealed, thus stripping away many of the confounding elements of context and communication known to influence trust (10). Volunteers were recruited from separate subject pools at Baylor College of Medicine in Houston, TX, and California Institute of Technology in Pasadena, CA. Volunteers were instructed identically, but separately, at each institution (instructors read a script describing the task).

We used event-related hyperscan-fMRI (h-fMRI) to monitor homologous regions of two subjects’ brains simultaneously as they played the multi-round trust game (19) (fig. S1). The motivating idea behind this approach is simple: To probe neural substrates of social interactions, we scan the brains of multiple subjects engaged in a social interaction. Social decision-making critically depends on internally represented models of social partners. In principle, such covert knowledge might be inferred from behavioral observations. However, behavioral signals are intrinsically lower dimensional than their underlying neural responses, and so behavior alone is an insufficient signal source for inferring neural representations. Put another way, an inference based only on the observable behavior of a social partner ignores many observable neural processes that give rise to that behavior. The measurement of both interacting brains directly sidesteps this problem and allows us to probe the cross correlation of internal models—replacing inference with a measurement.

Reciprocity predicts trust. Linear regression analyses of the behavior of 48 pairs of subjects identified reciprocity to be the strongest predictor of subsequent increases or decreases in trust (20). Reciprocity is defined as a fractional change in money sent across rounds by one

¹Human Neuroimaging Laboratory, Department of Neuroscience, ²Menninger Department of Psychiatry and Behavioral Sciences, Baylor College of Medicine, One Baylor Plaza, Houston, TX 77030, USA. ³Social Cognitive Neuroscience Laboratory, Division of Humanities and Social Sciences 228-77, California Institute of Technology, Pasadena, CA 91125, USA.

*To whom correspondence should be addressed.
E-mail: read@bcm.tmc.edu